PERGAMON

International Journal of Solids and Structures 38 (2001) 6839–6849

INTERNATIONAL JOURNAL OF SOLIDS and STRUCTURES

www.elsevier.com/locate/ijsolstr

Pressure and shear stress distributions of an elastomer constrained by a cylinder of finite length

Jang-Horng Yu [a], David A. Dillard [a,*], Didier R. Lefebvre [b]

[a] *Department of Engineering Science and Mechanics, Virginia Polytechnic Institute and State University, M/C 0219 Blacksburg, VA 24061, USA*

[b] *Automotive and Industrial Electronics Group, Motorola Corporation, Northbrook, IL 60062, USA*

Received 1 June 2000

Abstract

We study the pressure and shear stress response of an elastomer constrained by, and adhesively bonded to, a rigid cylinder of finite length and subject to different end boundary conditions. We find that the pressure and shear distributions are very sensitive to the compressibility of the elastomer as well as the aspect ratio of the cylinder. Notably, a slight change in the Poisson's ratio v has a profound effect on the pressure transmissibility of elastomers. Through this principle, we also propose using such geometries to measure the Poisson's ratio of elastomers, which is vital for engineers or designers who model the mechanical behavior of elastomers (e.g., rubbers or gels).

Keywords: Elastomer; Poisson's ratio; Bulk modulus; Experimental measurement; Shear lag; Gel

1. Introduction

The compressibility of polymers can affect the resulting stress distribution significantly, particularly for elastomeric materials where Poisson's ratio approaches 0.5. Schapery (see Lindsey (1967) for reference) studied the hydrostatic tension in polymers using a thin circular disk (poker chip), and showed that a small change in the Poisson's ratio v can alter the stress distribution significantly. Similar research can be found in Lai et al. (1992) who studied the response of an elastomeric block under a constrained configuration. Even a slight 0.1% change in v can cause a 35% change in the maximum pressure response.

Elastomers are often referred to as incompressible, a misconception arising from the fact that their Poisson's ratios approach a value of 0.5, the value of Poisson's ratio for truly incompressible materials. In fact, all elastomers are compressible; a rubbery polymer will be more compressible than the same polymer tested below the glass transition temperature, T_g, due to the decrease of its elastic modulus from a glassy state to a rubbery state. As with all isotropic continua, the bulk and shear moduli are given by

* Corresponding author. Tel.: +1-540-231-4714; fax: +1-540-231-9187.
E-mail address: dillard@vt.edu (D.A. Dillard).

0020-7683/01/$ - see front matter
PII: S0020-7683(01)00043-9

$$K = \frac{E}{3(1-2v)}, \qquad G = \frac{E}{2(1+v)}, \tag{1}$$

respectively, where E is the Young's modulus. Since v approaches 0.5 for elastomers, the bulk modulus is much greater than the shear modulus. For elastomeric components loaded with little constraint, the material deforms in distortion but does not significantly dilate or change volume. For more constrained applications, however, volume changes can be significant, and the assumption of incompressibility ($v = 0.5$) becomes highly inaccurate. For such geometries, small changes in Poisson's ratio can have dramatic effects on the resulting stress distributions and deformation fields.

Here, we illustrate the effect of compressibility of elastomers on their force transmissibility. We analyze the pressure and shear stress distributions within an elastomer that is constrained by and adhesively bonded to a rigid cylinder of finite length. Results show that the stress distribution resembles the classical Volkersen (1938) shear lag analysis.

Based on the pressure distribution of the elastomer, which is very sensitive to the Poisson's ratio of the material and the aspect ratio of the constrained cylinder, we have devised an experimental technique to measure the Poisson's ratio of elastomers and gels. This technique measures the pressure difference rather than the volume change for the material of interest. For gels, this technique is especially attractive because the related measurements for the volume change are hard to achieve. We have built a prototype of this device and preliminary experimental results seem promising (Dillard and Yu, 1999).

2. Constitutive assumptions and analysis

We consider an elastomeric rod constrained in a rigid cylindrical wall of radius a and depth H. The top surface sustains a uniform pressure p_0 and the bottom surface is either open or completely sealed (i.e., a rigid wall). The elastomer is assumed to be elastic and isotropic, and its bulk modulus K is much higher than the shear modulus G. We further assume that the elastomer is bonded to the cylinder wall permitting no relative movement, and the length of the cylinder is large compared to the radius of the cylinder so that the pressure p may be considered to be a function of the depth, or the axial direction, z, but independent of radius, i.e., $p = p(z)$.

Consider a circular disk element as shown in Fig. 1. In order to satisfy the force balance, we see that

$$p(\pi r^2) - (p + \mathrm{d}p)(\pi r^2) - \tau(2\pi r\,\mathrm{d}z) = 0, \tag{2}$$

which reduces to

$$\frac{\mathrm{d}p(z)}{\mathrm{d}z} = -\frac{2}{r}\tau. \tag{3}$$

If $u(r,z)$ is the deformation field, it relates to the shear stress τ via

$$\tau = G\frac{\partial u}{\partial r}. \tag{4}$$

Employing Eqs. (3) and (4) and noting that $u(r,z)|_{r=a} = 0$ since the material is bonded to the cylinder wall, we find that the deformation field $u(r,z)$ is parabolic:

$$u(r,z) = q(z)\left(1 - \frac{r^2}{a^2}\right), \tag{5}$$

where $q(z)$ is the (maximum) deflection of the elastomer at the center, and is of the form

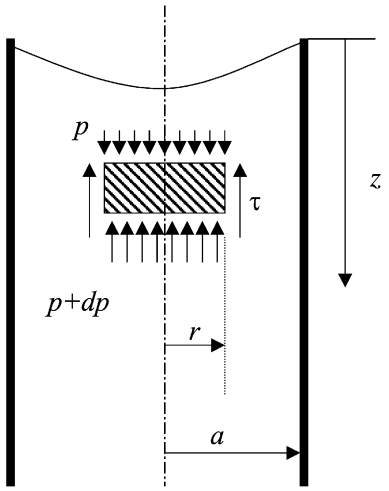

Fig. 1. Force balance of a circular disk element.

$$q(z) = \frac{a^2}{4G}\frac{\mathrm{d}p}{\mathrm{d}z}. \tag{6}$$

Note that Eq. (5) resembles that of a viscous fluid flowing through a pipe (see, e.g., Billington and Tate, 1981). Since $v \approx 0.5$, stresses in all directions are very similar for this constrained geometry, justifying the assumption of a hydrostatic pressure. Hence, we can calculate the volume change by

$$\Delta V(z) = \int_0^z \frac{p(\zeta)(\pi a^2)\,\mathrm{d}\zeta}{K}. \tag{7}$$

The volume change can be further expressed in the form

$$\Delta V(z) = \int_0^{q(z)} \pi a^2\left(1 - \frac{\zeta}{q(z)}\right)\mathrm{d}\zeta - \int_0^{q(H)} \pi a^2\left(1 - \frac{\zeta}{q(H)}\right)\mathrm{d}\zeta = \frac{\pi a^2(q(z) - q(H))}{2}, \tag{8}$$

where $q(H)$ is the axial deformation at the bottom of the elastomer. Combining Eqs. (7) and (8), we obtain the relation

$$q(z) - q(H) = \frac{2\int_0^z p(\zeta)\,\mathrm{d}\zeta}{K}. \tag{9}$$

This, with Eqs. (3) and (6), yields

$$\frac{\mathrm{d}p}{\mathrm{d}z} - \frac{8G}{Ka^2}\int_0^z p(\zeta)\,\mathrm{d}\zeta = \left.\frac{\mathrm{d}p}{\mathrm{d}z}\right|_{z=H}. \tag{10}$$

Differentiating Eq. (10) with respect to z will result in the following differential equation:

$$\frac{\mathrm{d}^2p}{\mathrm{d}z^2} - \lambda^2 p(z) = 0, \tag{11}$$

where

$$\lambda^2 \equiv \frac{8G}{Ka^2}. \tag{12}$$

The solutions for Eq. (11) are clearly of the form sinh( ) and cosh( ), where

$$p(z) = A\sinh\left(\bar{\lambda}\left(\frac{z}{H}-1\right)\right) + B\cosh\left(\bar{\lambda}\left(\frac{z}{H}-1\right)\right), \tag{13}$$

and by Eqs. (1) and (12) we denote the non-dimensional parameter

$$\bar{\lambda} = \lambda H = \sqrt{\frac{8G}{K}}\frac{H}{a} = \sqrt{\frac{12(1-2\nu)}{(1+\nu)}}\frac{H}{a}. \tag{14}$$

A and B are integration constants determined by the boundary conditions. In the following, we shall apply different traction or displacement constraints to solve for the stress and pressure distribution within the elastomer for several configurations of interest.

2.1. Cylinder with a sealed end

In this section, we consider the case of a cylinder with a sealed lower end, and the elastomer sustains a pressure p_0 at the top surface. Employing the boundary conditions where $q(H) = 0$, we readily find that the normalized pressure distribution and the corresponding shear stress are, respectively, of the forms

$$\frac{p(z)}{p_0} = \frac{\cosh(\bar{\lambda}(\frac{z}{H}-1))}{\cosh(\bar{\lambda})}, \tag{15}$$

$$\frac{\tau(r,z)}{p_0} = -\frac{\frac{r}{a}\sqrt{\frac{3(1-2\nu)}{(1+\nu)}}\sinh(\bar{\lambda}(\frac{z}{H}-1))}{\cosh(\bar{\lambda})}. \tag{16}$$

We hence conclude that the pressure and shear stress distribution depend on the compressibility of the material ν as well as the geometric configurations of the cylinder H/a. In addition, the shear stress is linear along the radial direction r.

Next, we shall plot the pressure and shear distribution along the axial direction z. For the shear stress, we shall calculate the shear stress at the cylinder wall, τ_w, where we set $\tau_w \equiv \tau(a,z)$. Fig. 2 shows a plot of pressure ratio p/p_0 distribution and shear stress at the cylinder wall τ_w/p_0 for different values of ν. Clearly, if ν is closer to 0.5, we see less change in the pressure profile. For smaller values of ν's, the pressure drops more significantly because the material is more compressible. Fig. 3 shows a plot of pressure ratio p/p_0 distribution and shear stress at the cylinder wall τ_w/p_0 for different values of the characteristic length H/a. We observe a similar effect of an increasing of H/a to a decrease in ν. The initial decreasing rate of pressure is more significant for large values of H/a. Fig. 4 shows the values of the bottom pressure p_b/p_0 vs. H/a for different Poisson's ratios.

2.2. Cylinder with open surfaces

In this section, we consider the case of a cylinder with free top and bottom surfaces while the elastomer sustains top and bottom pressures p_0 and p_b, respectively. In this case, invoking the boundary conditions where $p(0) = p_0$ and $p(H) = p_b$, we will obtain

$$p(z) = \frac{\left[-p_0 + \frac{p_b}{\cosh(0)}\cosh(\bar{\lambda})\right]}{\sinh(\bar{\lambda})}\sinh\left(\bar{\lambda}\left(\frac{z}{H}-1\right)\right) + \frac{p_b}{\cosh(0)}\cosh\left(\bar{\lambda}\left(\frac{z}{H}-1\right)\right), \tag{17}$$

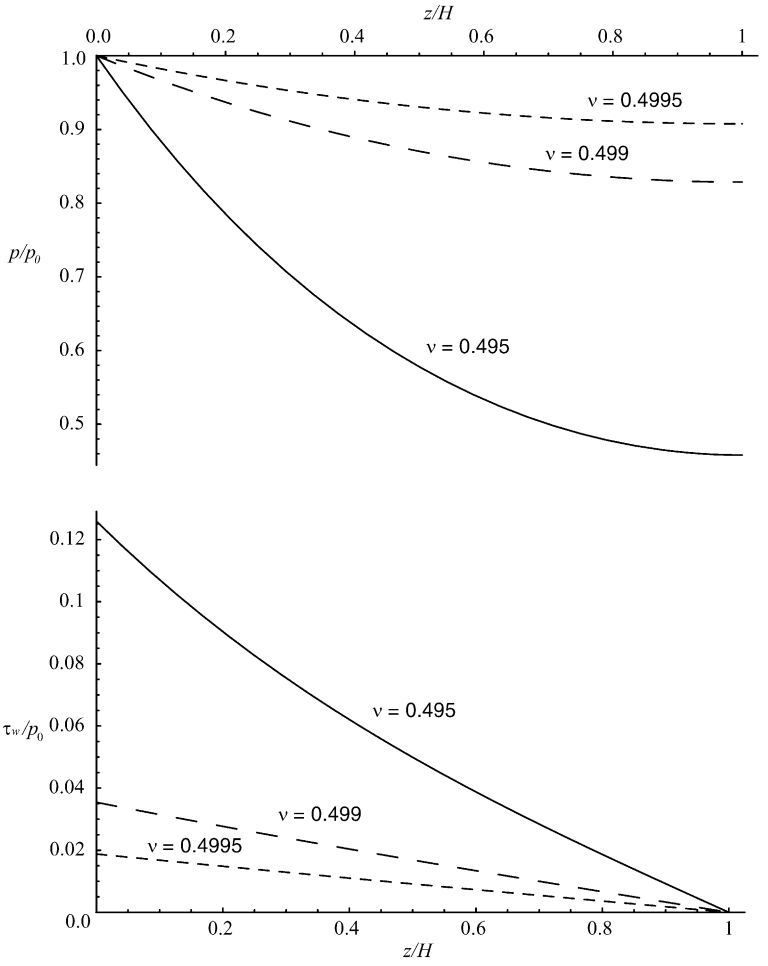

Fig. 2. Pressure transmission and shear stress vs. depth for different values of Poisson's ratio for the case $H/a = 5$.

$$\tau(r,z) = \frac{\frac{r}{a}\sqrt{\frac{3(1-2\nu)}{(1+\nu)}}\left[p_0 - \frac{p_b}{\cosh(0)}\cosh(\bar{\lambda})\right]}{\sinh(\bar{\lambda})}\cosh\left(\bar{\lambda}\left(\frac{z}{H}-1\right)\right) - \frac{r}{a}\sqrt{\frac{3(1-2\nu)}{(1+\nu)}}\frac{p_b}{\cosh(0)}\sinh\left(\bar{\lambda}\left(\frac{z}{H}-1\right)\right). \tag{18}$$

If the bottom surface is also pressure-free, the solution will reduce to

$$\frac{p(z)}{p_0} = -\frac{\sinh(\bar{\lambda}(\frac{z}{H}-1))}{\sinh(\bar{\lambda})}, \tag{19}$$

$$\frac{\tau(r,z)}{p_0} = \frac{\frac{r}{a}\sqrt{\frac{3(1-2\nu)}{(1+\nu)}}\cosh(\bar{\lambda}(\frac{z}{H}-1))}{\sinh(\bar{\lambda})}. \tag{20}$$

In the following, we plot the pressure and shear distribution along the axial direction for an open cylinder with different applied pressures. Fig. 5 shows a plot of pressure ratio p/p_0 distribution and shear stress

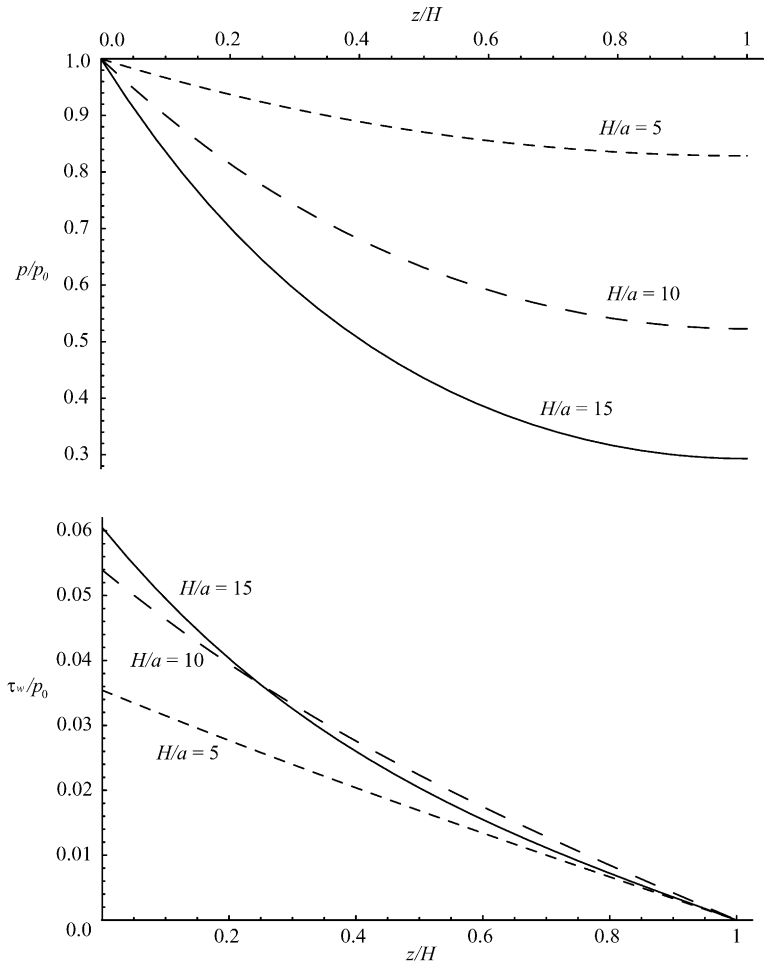

Fig. 3. Pressure transmission and shear stress vs. depth for different ratios of H/a for the case $v = 0.499$.

at the cylinder wall τ_w/p_0 for different values of v under applied pressures $p_b/p_0 = 0.2$. Clearly, if v is closer to 0.5, we will see the pressure profile vs. depth is almost linear. For smaller values of v's, the pressure drops more rapidly in the beginning because the material is more compressible. In Fig. 6, we plot the pressure profiles and shear stress at the cylinder wall for different ratios of H/a under applied pressures $p_b/p_0 = 0.1$. We note that if the value H/a is large enough, the pressure actually undershoots before it comes back to satisfy the boundary conditions because of the sign change of the shear stress. Such undershoots are expected for sufficiently long or significantly compressible scenarios.

3. Comparison with finite element analysis

In order to determine the accuracy of the analytical solutions where p is used as the hydrostatic pressure to calculate the volume change and is of the form $p = p(z)$, we provide in this section a com-

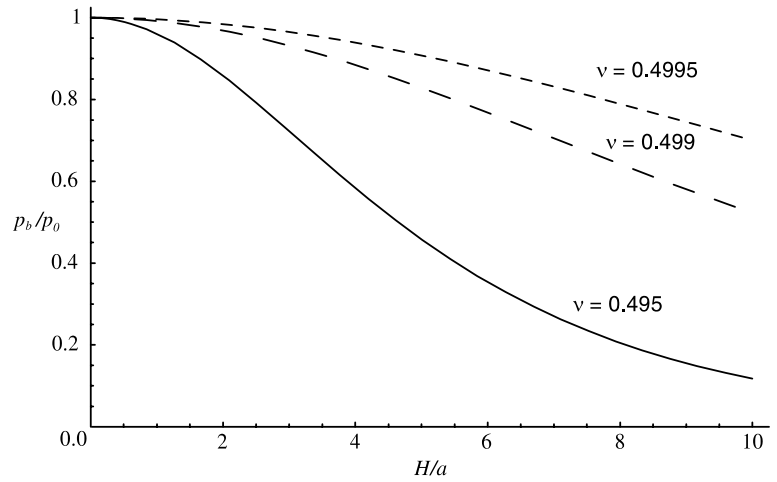

Fig. 4. Pressure transmission at the bottom of the cylinder for different values of H/a and v.

parison between finite element analysis (FEA) results and the closed form solution. A 2D axisymmetric FEA model representing half of the confined gel body is built in ANSYS, as shown in Fig. 7. A half model is chosen due to the symmetry in geometry and loading conditions. Rigid walls are modeled by fixing the displacement at the boundaries to null. We use eight-node quadratic elements for the analysis. The element size near the walls of the tube is reduced to capture the high shear stress gradients near the tube boundaries. We change the aspect ratio of the tube by varying the height H while maintaining the radius $a = 10$ mm.

We analyze the cases of open-end and closed-end configurations with different ratios of H/a where the bulk modulus and shear modulus of a specific gel are given by $K = 100$ MPa and $G = 0.06$ MPa, respectively, which corresponds to the value of Poisson's ratio $v = 0.4997$. Because the Poisson's ratio is close to 0.5, we use an incomplete Cholsky conjugate gradient (ICCG) solver to achieve convergence. We shall illustrate the accuracy of the closed form solution, especially the assumption that $p = p(z)$ by choosing different characteristic lengths of the cylinder H/a for both configurations.

In Figs. 8 and 9, we provide a comparison of the pressure distribution within the elastomer for the FEA results and the closed form solution. In a closed cylinder where the motion is highly constrained, the analytical solution is observed to be below the FEA results for large values of H/a. This is probably because we calculate the volume change (8) by assuming $p(z)$ is the hydrostatic pressure; hence ΔV is slightly larger than the real situation. This implies that the pressure drop will be more pronounced than in reality because the elastomer appears to be more compressible. In an open cylinder, however, the pressure profile from FEA tends to be below the analytical solution as z/H increases. This may be due to the fact that the deformation is less constrained and the shear stress distribution may not obey relationship (20). Nevertheless, the FEA results and the closed form solutions are in good agreement for both cases.

We note from the above analysis that the pressure and shear distributions are indeed very sensitive to the volume change, which depends on the shape of the deformed surfaces. Assuming the case that $p = p(z)$ will yield a parabolic deformed surface. For shallow cylinders, however, where H and a are comparable, one should treat $p = p(r, z)$, for which the analytical solutions would be much harder to derive, and the deformed surface will not be parabolic in shape. We shall also note that, for the case of hydrostatic tension in poker chip specimens, the stress solution is given by modified Bessel functions of the radius r where the thickness effect is neglected (Lindsey, 1967). For our study on the long constrained elastomeric cylinders

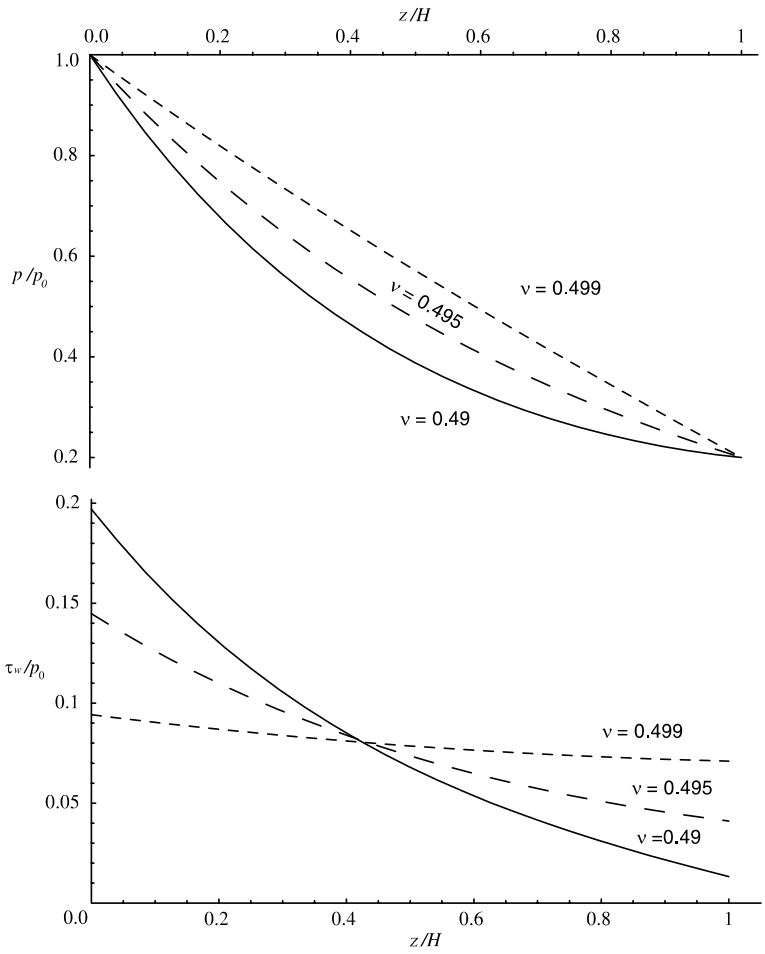

Fig. 5. Pressure transmission and shear stress vs. depth for different values of Poisson's ratio for the case $H/a = 5$ and $p_b/p_0 = 0.2$.

where the radius dependence is neglected, the pressure solution is given by sinh and cosh functions of the depth z.

4. Potential applications to experimentally evaluate v

The closed form solution Eq. (15) not only calculates the pressure profile $p(z)/p_0$, but also suggests an alternative means to measure v or K (assuming G is known) for elastomers without directly measuring the volume change. Instead, the pressure difference measured at different positions of an elastomer-filled cylinder can be used to determine v. Different geometric configurations, e.g., cylinders of different sizes or boundary conditions, may be used to improve the accuracy of the measurement (Dillard and Yu, 1999).

The experimental determination of material constants v and K for elastomers is known to be a delicate and difficult task. Such experimental procedures often require expensive apparatus and are prone to error due to the fact that the volume change for elastomeric materials is very small. Furthermore, a very small change in v will produce a drastic change in K.

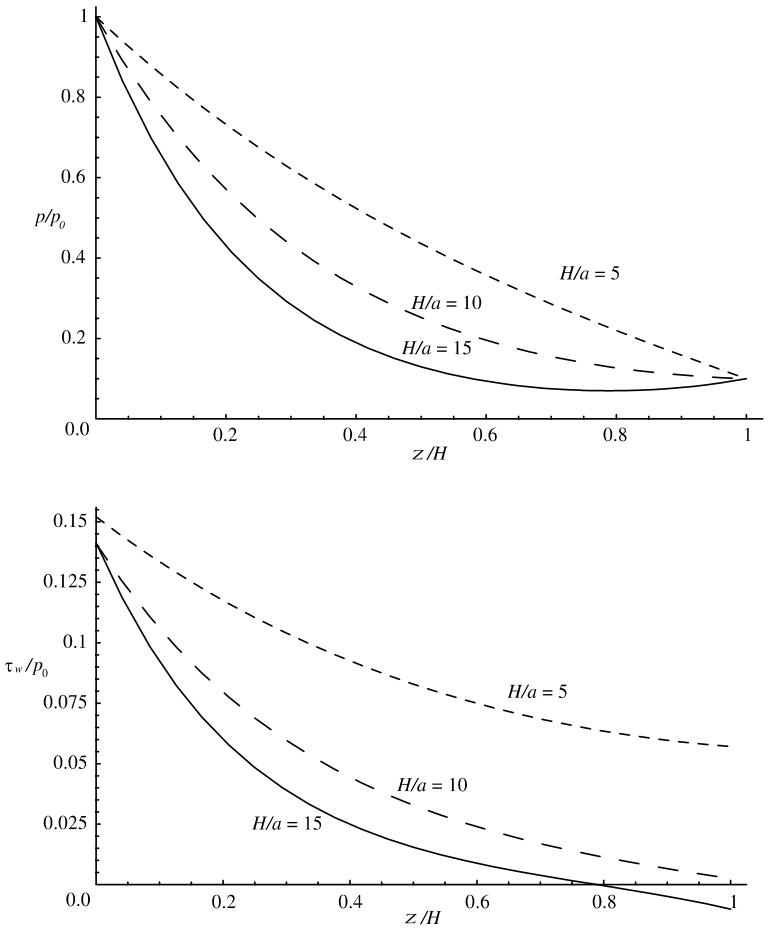

Fig. 6. Pressure transmission and shear stress vs. depth for different ratios of H/a for the case $v = 0.495$ and $p_b/p_0 = 0.1$.

Here, the Poisson's ratio is indirectly measured via the pressure difference. Such experiments would be easy and inexpensive to perform. The fact that there is no moving part required in the experiment would make this technique more reliable and repeatable.

5. Conclusions

Elastomers are widely used as damping materials, sealants, and force transmitters, just to name a few. We have shown that the force response of the elastomer is very sensitive to its compressibility, especially when the motion is constrained. A slight decrease in v can drastically attenuate the pressure transmission. This phenomenon can have a profound effect on the applications and mechanical designs of such materials involving force transmissibility in constrained deformations.

The mechanical properties of elastomers depend on their material constants K, G or v. The experimental technique using the pressure difference to measure the Poisson's ratio and other bulk material properties will provide crucial experimental data for designers and engineers, in addition to the fundamental analysis and understanding of the stress distribution within elastomers.

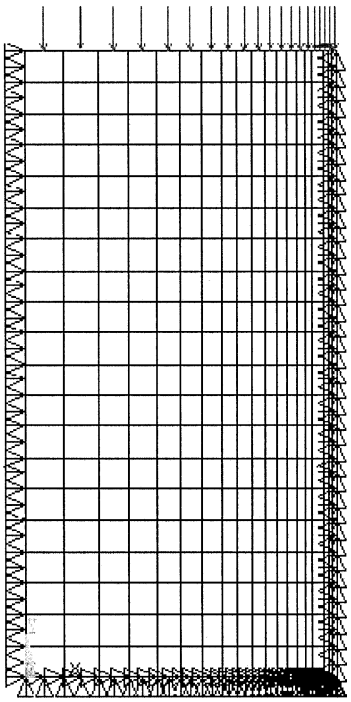

Fig. 7. Mesh and boundary conditions for a closed cylinder with $H/a = 2$.

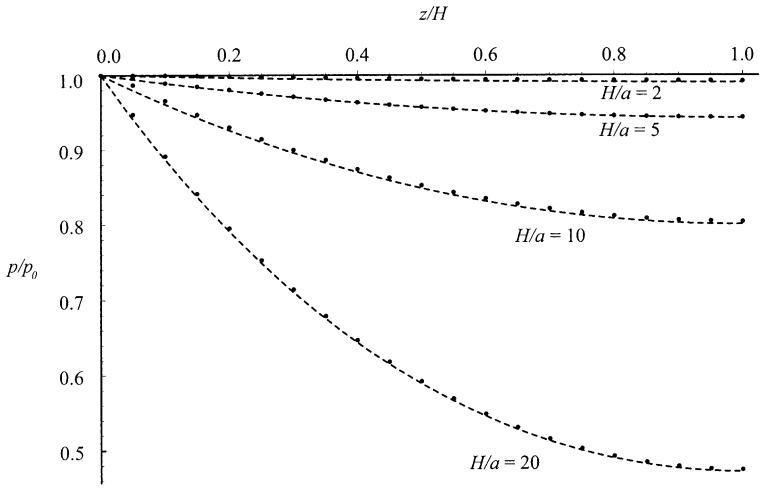

Fig. 8. Comparison of FEA results and closed form solutions for a closed cylinder with different values of H/a for $v = 0.4997$. The FEA data is indicated as dots.

Acknowledgements

We gratefully acknowledge the support of NSF-STC #DMR 9120004, the Center for Adhesive and Sealant Science, and the Department of Engineering Science and Mechanics.

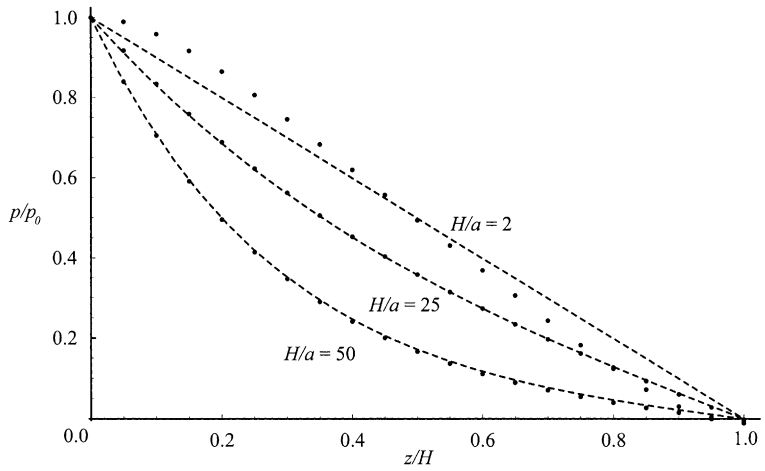

Fig. 9. Comparison of FEA results and closed form solutions for an open cylinder with different values of H/a for $v = 0.4997$. The FEA data is indicated as dots.

References

Billington, E.W., Tate, A., 1981. The Physics of Deformation and Flow. McGraw Hill, New York.

Dillard, D.A., Yu, J.H., 1999. Experimental Measurements of Poisson's Ratio for Elastomers and Gel-like Polymers. Patent Disclosure, Virginia Tech Intellectual Property 99.064.

Lai, Y.H., Dillard, D.A., Thornton, J.S., 1992. J. Appl. Mech. 59, 902–908.

Lindsey, G.M., 1967. J. Appl. Phys. 38 (12), 4843–4852.

Volkersen, O., 1938. Luftfahrforschung 15, 41.